Hydrograph separation using tracers and digital filters to quantify runoff components in a semi-arid mesoscale catchment

Saraiva Okello, Aline Maraci Lopes; Uhlenbrook, Stefan; Jewitt, Graham P.W.; Masih, Ilyas; Riddell, Edward Sebastian; Van der Zaag, Pieter

DOI
10.1002/hyp.11491

Publication date
2018

Document Version
Final published version

Published in
Hydrological Processes

Citation (APA)
Saraiva Okello, A. M. L., Uhlenbrook, S., Jewitt, G. P. W., Masih, I., Riddell, E. S., & Van der Zaag, P. (2018). Hydrograph separation using tracers and digital filters to quantify runoff components in a semi-arid mesoscale catchment. *Hydrological Processes*, *32*(10), 1334-1350. https://doi.org/10.1002/hyp.11491

Received: 15 August 2017 | Accepted: 16 February 2018
DOI: 10.1002/hyp.11491

RESEARCH ARTICLE

WILEY

Hydrograph separation using tracers and digital filters to quantify runoff components in a semi-arid mesoscale catchment

Aline Maraci Lopes Saraiva Okello[1,2] | Stefan Uhlenbrook[1,3,4] | Graham P.W. Jewitt[2,5] | Ilyas Masih[1] | Edward Sebastian Riddell[2] | Pieter Van der Zaag[1,3]

[1] IHE, Delft, The Netherlands

[2] University of KwaZulu-Natal, Centre for Water Resources Research, Pietermaritzburg, South Africa

[3] Section of Water Resources, Delft University of Technology, Delft, The Netherlands

[4] UN World Water Assessment Programme (WWAP), UNESCO, Perugia, Italy

[5] Umgeni Water Chair of Water Resources Management, University of KwaZulu-Natal, Pietermaritzburg, South Africa

Correspondence
Aline Maraci Lopes Saraiva Okello, IHE, Delft, The Netherlands.
Email: a.saraiva@un-ihe.org

Funding information
Schlumberger Foundation, Grant/Award Number: Faculty of the Future Fellowship 2014-2015; L'Oreal-UNESCO "For Women in Science, Sub-Saharan Africa 2013"; Water Research Commission of South Africa, Grant/Award Number: K5/1935; RISKOMAN

Abstract

Chemical hydrograph separation using electrical conductivity and digital filters is applied to quantify runoff components in the 1,640 km^2 semi-arid Kaap River catchment and its subcatchments in South Africa. A rich data set of weekly to monthly water quality data ranging from 1978 to 2012 (450 to 940 samples per site) was analysed at 4 sampling locations in the catchment. The data were routinely collected by South Africa's national Department of Water and Sanitation, using standard sampling procedures. Chemical hydrograph separation using electrical conductivity (EC) as a tracer was used as reference and a recursive digital filter was then calibrated for the catchment. Results of the two-component hydrograph separation indicate the dominance of baseflow in the low flow regime, with a contribution of about 90% of total flow; however, during the wet season, baseflow accounts for 50% of total flow. The digital filter parameters were very sensitive and required calibration, using chemical hydrograph separation as a reference. Calibrated baseflow estimates ranged from 40% of total flow at the catchment outlet to 70% in the tributaries. The study demonstrates that routinely monitored water quality data, especially EC, can be used as a meaningful tracer, which could also aid in the calibration of a digital filter method and reduce uncertainty of estimated flow components. This information enhances our understanding of how baseflow is generated and contributed to streamflow throughout the year, which can aid in quantification of environmental flows, as well as to better parameterize hydrological models used for water resources planning and management. Baseflow estimates can also be useful for groundwater and water quality management.

KEYWORDS

digital filters, hydrograph separation, runoff generation, semi-arid catchment, Southern Africa, tracers

1 | INTRODUCTION

Hydrological processes, particularly runoff generation, influence water quality and water quantity as well as their spatial and temporal dynamics. Detailed understanding of these processes is thus important for the prediction of water resources yield, floods, erosion, and solute and contaminant transport (Blöschl, Sivapalan, Wagener, Viglione, & Savenije, 2013; Hrachowitz et al., 2011). The recent concluded IAHS decade of Prediction of Ungauged Basins (Hrachowitz et al., 2013) and the current decade "Panta Rhei-everything flows" (Montanari

et al., 2013) stress the importance of making better use of all available data and combining different methods in order to get a more holistic understanding of catchment functioning and hydrological processes.

Semi-arid systems, which constitute a large part of the African continent, are characterized by high spatio-temporal variability of rainfall, high evaporation rates, deep groundwater resources, and poorly developed soils (Blöschl et al., 2013; Hrachowitz et al., 2011; Hughes, 2007; Wheater, Sorooshian, & Sharma, 2008). Additionally, semi-arid systems have marked seasonality and are more prone to flood and drought extremes, with dry spells that can last for years (Love, Uhlenbrook, Corzo-Perez, Twomlow, & van der Zaag, 2010). High-intensity storms may generate most of the season's runoff (Love et al., 2010; Van Wyk, Van Tonder, & Vermeulen, 2012). These characteristics, combined with the multiple other challenges such as growing population, increasing water use and irrigation, urbanization, and pollution, make it extremely important to better understand runoff generation in semi-arid areas (Hughes, 2007).

There is no standard procedure to best understand runoff generation processes (Beven, 2012), but several methods are often applied to quantify runoff components, including graphic hydrograph separation, rainfall–runoff models, baseflow filters, and chemical/isotope (tracer) hydrograph separation (Cartwright, Gilfedder, & Hofmann, 2014; Gonzales, Nonner, Heijkers, & Uhlenbrook, 2009; Uhlenbrook, Frey, Leibundgut, & Maloszewski, 2002; Zhang, Li, Chow, Li, & Danielescu, 2013). Hydrograph separation is commonly applied to quantify different components contributing to river flow. River discharge following a rainfall event may be divided into quickflow and baseflow (Hall, 1968; Stewart, 2015; Tallaksen, 1995). Quick flow is the water that contributes to river flow immediately after the rainfall event, but it can include water from different sources (Cartwright et al., 2014; Hrachowitz et al., 2011), such as rainfall, overland flow, and older water displaced from unsaturated or saturated zone (Cartwright et al., 2014; Sklash & Farvolden, 1979). Baseflow is water with longer response time to precipitation in the catchment which sustains the river between rainfall events and seasons. It can include contributions from regional groundwater, interflow, water from river banks, and floodplains (Cartwright et al., 2014; Sklash & Farvolden, 1979; Tallaksen, 1995). Therefore, these components can be made up of water from different sources, the contributions of which vary in space and time, and further complicate the understanding of underlying processes (Cartwright et al., 2014).

Hydrological process studies are costly and labour intensive (Hughes, Hannart, & Watkins, 2003; Hughes, Jewitt, Mahé, Mazvimavi, & Stisen, 2015; Wenninger, Uhlenbrook, Lorentz, & Leibundgut, 2008). In addition, there is often limited capital and human resources to perform them, particularly in the poorly gauged catchments of Africa (Hughes et al., 2003; Hughes et al., 2015). The use of tracers in such situations has been shown to be a cost-effective and a pragmatic approach. Indeed, several recent studies show the potential of using tracers to improve the understanding of runoff generation processes and flow paths in small catchments (Birkel, Soulsby, & Tetzlaff, 2014; Birkel, Tetzlaff, Dunn, & Soulsby, 2010; Capell, Tetzlaff, Malcolm, Hartley, & Soulsby, 2011; Capell, Tetzlaff, & Soulsby, 2012; Tetzlaff & Soulsby, 2008; Wenninger et al., 2008). However, such studies at a larger scale (e.g., $>10^3$ km^2) are still rare (Frisbee, Phillips, White, Campbell, & Liu, 2013; Miller, Johnson, Susong, & Wolock, 2015; Miller, Susong, Shope, Heilweil, & Stolp, 2014; Tetzlaff et al., 2015), as many factors influence water quality at the catchment scale, such as geology, soils, elevation, topography, climate, seasonality, and land use management.

For hydrograph separation to be useful, tracers should be conservative and not react during their medium of transport through the catchment. This is mostly the case with environmental tracers, such as deuterium and oxygen-18 (Klaus & McDonnell, 2013). However, historical data on the concentration of these conservative tracers in the catchment are generally not available; therefore, hydrochemical tracers are used for hydrograph separation. Several studies (Capell et al., 2011; Miller et al., 2014; Miller et al., 2015; Soulsby et al., 2004; Tetzlaff & Soulsby, 2008; Uhlenbrook et al., 2002) have used electrical conductivity (EC), alkalinity, chloride, and silica as tracers to perform hydrograph separation, despite some limitations. Authors argue that different tracers contain different information, for instance, silica can be a good tracer of geographical sources of runoff (Uhlenbrook et al., 2002), whereas alkalinity could be used as a conservative tracer to differentiate between acidic soil–water and more alkaline groundwater (Tetzlaff & Soulsby, 2008; Tetzlaff, Waldron, Brewer, & Soulsby, 2007). Uhlenbrook et al. (2002) used dissolved silica concentration as an indicator of residence time of water and infer the source and pathway for runoff components. In that study, overland flow from saturated and impervious areas of the Brugga catchment in Germany were assumed to have no dissolved silica (resembling rainfall) whereas, in subsurface flow components, the water had time to react with mineral soil and become enriched with dissolved silica depending on the geology and residence time of the water.

A recursive digital filter is a method adapted from signal processing theory (Eckhardt, 2005; Nathan & McMahon, 1990). In application of this method, daily stream flow time series are considered a mixture of quickflow (high-frequency signal) and baseflow (low-frequency signal). By filtering out the high-frequency signals from the streamflow, the low-frequency signals (baseflow) can be revealed. Recursive digital filters have been applied for graphical hydrograph separation (Cartwright et al., 2014; Eckhardt, 2005; Eckhardt, 2008; Miller et al., 2015), using only streamflow records and filter parameters, which can be calibrated with tracer data (Longobardi, Villani, Guida, & Cuomo, 2016; Rimmer & Hartmann, 2014; Zhang et al., 2013) or other catchment characteristics (Cartwright et al., 2014; Eckhardt, 2005; Mei & Anagnostou, 2015). Some recent studies have shown the potential of combining hydrochemical tracer, particularly EC, and digital filter methods in order to estimate baseflow for long records of streamflow (Li et al., 2014; Longobardi et al., 2016; Miller et al., 2014; Miller et al., 2015; Rimmer & Hartmann, 2014; Zhang et al., 2013). Hydrograph separation using calibrated digital filters is therefore inexpensive and allows for quick and objective separation of streamflow components, which are important in the management of water resources. However, this approach has not been tested extensively in arid and semi-arid systems, particularly in Southern Africa.

Building from this body of literature, the main objective of this paper is to use water quality data, especially EC, and a digital filter

hydrograph separation method to quantify runoff components in a semi-arid catchment in Southern Africa. EC was chosen as main tracer because it is easy and cheap to measure and widely available; therefore, its applicability is important to understand. Depending on geology, other tracers such as dissolved silica (e.g., Uhlenbrook and Hoeg (2003)) can be useful. However, due to availability, this study focused on the examining the potential of EC as tracer.

Thus, the specific objectives are to:

- assess if long-term discrete EC data can be used to perform hydrograph separation at the monthly scale in a mesoscale semi-arid catchment;
- perform hydrograph separation using digital filters at daily timescale and assess the methodology to calibrate filter parameters using EC data; and
- quantify the relative contribution of quickflow and baseflow to total runoff at both monthly and annual timescales.

2 | METHODOLOGY

2.1 | Study area—The Kaap catchment

The Kaap catchment is located in the northeast of South Africa in the Mpumalanga province and drains an area of approximately 1,640 km^2. Flowing from west to east, the Kaap River joins the Crocodile River which then flows to the transboundary Incomati River. The Kaap catchment contains three main tributaries: the Queens, the Suidkaap, and the Noordkaap (see Figure 1. and Table 1). The study area is located in the low elevation subtropical region of South Africa, Swaziland, and Mozambique known as the Lowveld with elevations ranging from 300 to 1,800 m above sea level (see Figure 1.a). The climate is semi-arid with cool dry winters and hot wet summers, characterized by a distinct wet and dry season, with significant intraseasonal variability associated with the summer rainfall season which is dominated by thermal and orographic thunderstorms. The wet season typically runs from October to March, as illustrated in Figure 2. Precipitation ranges from 583 to 1243 mm/y in the highest parts of the catchment (Middleton & Bailey, 2009). The mean potential evaporation is estimated to 1435 mm/y (Middleton & Bailey, 2009).

Streamflow is highly seasonal with the highest average flow occurring in February with an average of 9.2 m^3/s at the outlet and a mean annual runoff coefficient of 0.14. The lowest flow during the year is observed at the end of the dry season in September falling to an average of 0.8 m^3/s. Minimum and maximum mean daily flows recorded between 1961 and 2012 at the Kaap outlet range from 0 (below detection limit) to 483 m^3/s. The catchment is fairly well monitored with five streamflow gauges available within the catchment (see Figure 1.a). According to Bailey and Pitman (2015), the long-term natural mean annual runoff of the Kaap River catchment is $189 \cdot 10^6$ m^3/y (equivalent to 116 mm/y). Table 1 describes the physiographic characteristics of the Kaap and tributaries in more detail. Woody savannah (Bushveld) and grasslands are the dominant land cover in the Kaap Valley covering up to 68% of the catchment as observed in Figure 1. b and Table 1. In the upstream areas, approximately a quarter of the total catchment consists of exotic pine and eucalyptus plantations used for paper and timber production. Sugarcane, vegetables, and citrus orchards are found downstream and are irrigated. No other major structures, such as reservoirs, are present in the catchment. The total population of the Umjindi municipality (which cover most of the Kaap catchment) is over 71,200, distributed between the town of Barberton (over 12,000) and several townships, farms, and informal settlements (Stats S, 2016). There are some gold mines still active in the catchment.

The Kaap valley presents some of the oldest rock formations on Earth, including the Onverwacht group, some 3.5 billion years old (de Wit, Furnes, & Robins, 2011; Sharpe et al., 1986). Biotite granite is the predominant formation in the valley as observed in Figure 1.c. The headwaters originate over the weathered granite which has felsic properties indicating high concentrations of silica (Hessler & Lowe, 2006). In contrast, surrounding the granite, lava formations are present in the form of basalt and peridotitic komatiite which are low in silicates and high in magnesium. Sandstones and shales are found in proximity to the Kaap River and at the south section of the catchment (Hessler & Lowe, 2006; Sharpe et al., 1986). In addition to the gneiss formation observed at the outlet, other formations present include ultramafic (high in iron and low silicates) rocks, quartzite, and dolomite (see Figure 1.c and Table 1).

The predominant soils are rhodic ferrasols, chromic cambisols, and haplic acrisols in the headwater catchments. In the Kaap valley, lithic leptosols and rhodic nitisols dominate (Hengl et al., 2014; Hengl et al., 2017). In terms of soil texture, 53% of the Kaap catchment is covered in sandy clay loams, 39% in clay loams, and the remainder of the catchment has clays, sandy clays and sandy loams (Hengl et al., 2014; Hengl et al., 2017).

2.2 | Data used

Hydrological data in the catchment including precipitation, evaporation, streamflow, and groundwater records were collected from the South African Department of Water & Sanitation (DWS, former DWA), the South African Weather Service (SAWS), and the South African Sugarcane Research Institute. Geological, topographical, and land use data were obtained from the Middleton and Bailey (2009) and the Catchment Management Strategy studies (ICMA, 2010). To analyse the flow behaviour at the outlet and tributaries, average daily discharges at X2H022 (Outlet), X2H008 (Queens), X2H031 and X2H024 (Suidkaap), and X2H010 (Noordkaap) stream gauges were obtained from the DWS. Their locations are shown in Figure 1.a. Time series of water quality (Electrical conductivity, pH, Calcium, Magnesium, Potassium, Sodium, Chloride, Sulphates, Total Alkalinity, Silica, Fluoride, Nitrates, Ammonia, Phosphate and Total Dissolved Salts) were obtained from the DWS Water Management System (https://www.dwa.gov.za/iwqs/wms/). The time series of water quality is intermittent, with weekly or fortnightly samples in some years and monthly samples in others. Rainfall water quality was not part of the routine sampling programme undertaken by DWS. Table 2 details the location, time series length, and source of data used.

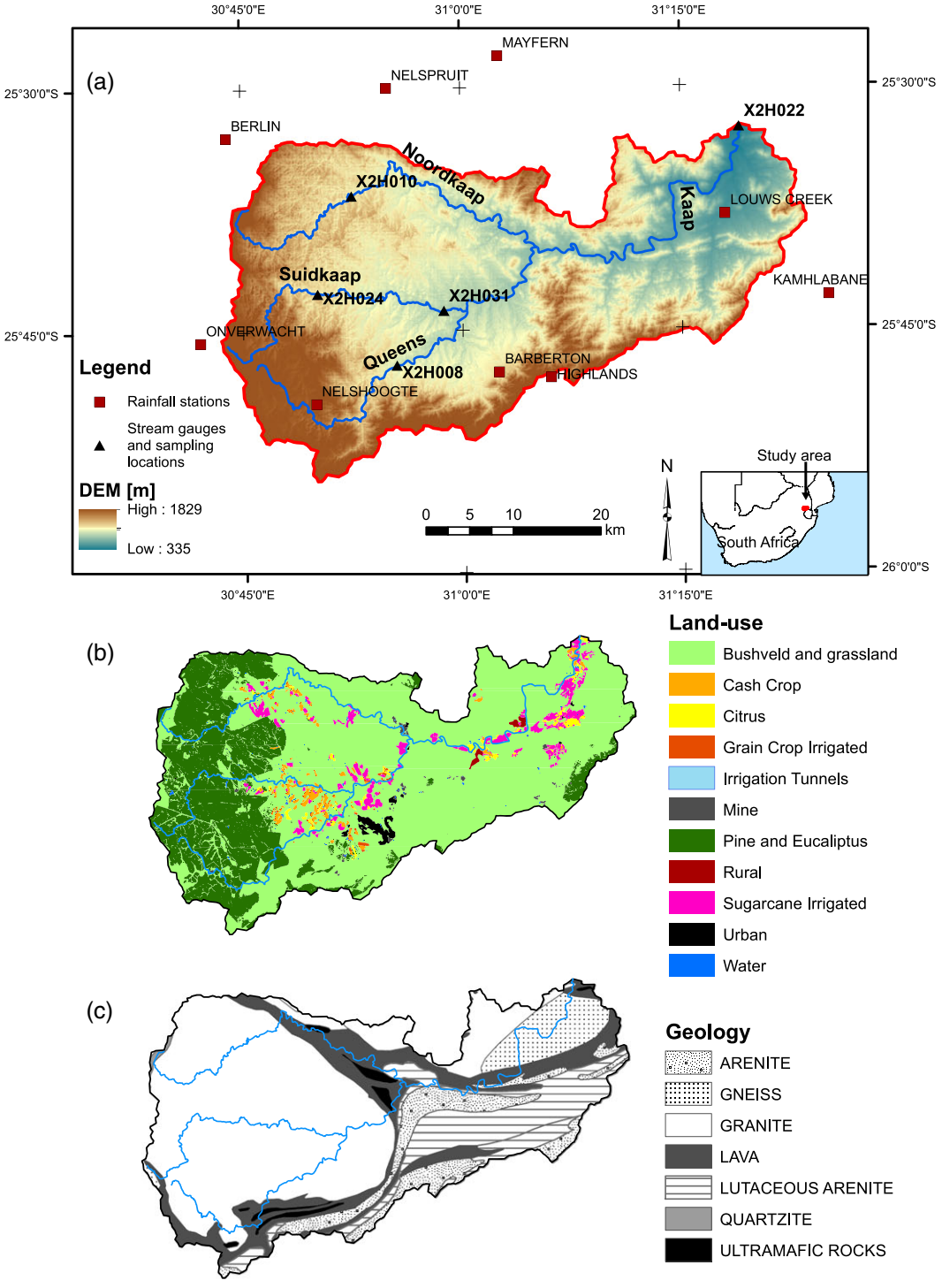

FIGURE 1 (a) Location of Kaap catchment in South Africa (inset) and DEM of Kaap catchment with sampling locations, stream gauges and rainfall stations, (b) land-use and land-cover map of Kaap catchment, and (c) geological map (Middleton and Bailey, 2009)

2.3 | Chemical hydrograph separation

EC data were combined with discharge data to perform a two-component hydrograph separation based on steady state mass balance equations of water and tracer fluxes, as described by Equations 1 and 2.

$$Q_t = Q_s + Q_b, \tag{1}$$

$$c_t\, Q_t = c_s\, Q_s + c_b Q_b, \tag{2}$$

where Q_t is mean daily discharge at sampling point (m^3/s), Q_s is the runoff contribution from the surface runoff (m^3/s) and Q_b is the runoff contribution from the subsurface runoff (m^3/s); c_t is the tracer concentration at the sampling point (μS/cm);, c_s is the tracer concentration of the surface runoff (μS/cm) and c_b is the tracer concentration of the subsurface runoff (μS/cm).

The concentration for subsurface runoff was assumed to be the concentration of streamflow when the flow is lowest (assuming these are baseflow conditions) and the concentration of the surface runoff

TABLE 1 Catchment physiographic and hydroclimatic characteristics

Tributary name	Kaap outlet	Queens	Suidkaap	Noordkaap
Hydrometric station ID	X2H022	X2H008	X2H031	X2H010
Sub-basin area, km^2	1640	180	262	126
Reach length up to station, km	108	30	41	25
Topography				
Mean elevation, m.a.s.l	899	1261	985	1090
Min elevation, m.a.s.l	332	733	651	847
Max elevation, m.a.s.l	1862	1688	1862	1755
Mean slope, degrees	11	11	7	9
Max slope, degrees	60	51	45	57
Geology				
Granite, %	53	60	98	97
Lava, %	16	28	1	0
Arenite, %	9	2	0	0
Ultramafic, %	2	4	0	0
Quartzite, %	0	0	0	3
Gneiss, %	6	0	1	0
Lutaceous arenite, %	14	6	0	0
Land use (2004; Middleton and Bailey, 2009)				
Bushveld and grassland, %	67.6	36.3	37.1	30.0
Planted forest (pine and eucalyptus), %	25.0	63.5	55.6	68.4
Irrigated cultures (sugarcane, citrus, others), %	6.0	0.0	7.0	1.6
Urban and mines, %	1.4	0.1	0.4	0.1
Hydro-meteorology				
Mean annual precipitation from 1950–2010, mm/y	900	1016	905	1101
Potential ET (S-Pan), mm/y	1435	1369	1451	1425
Runoff (MAR) natural (WR2012, 1970–2010), mm/y	116	146	210	216
Runoff (MAR) observed (1970–2010), mm/y	66	99	120	149
Qmin, m^3/s	0	0	0	0
Q95, m^3/s	0.01	0.02	0.12	0.12
Qmean, m^3/s	1.35	0.25	0.61	0.40
Q5, m^3/s	13.18	2.05	2.89	1.58
Qmax, m^3/s	482.63	95.88	123.35	27.93

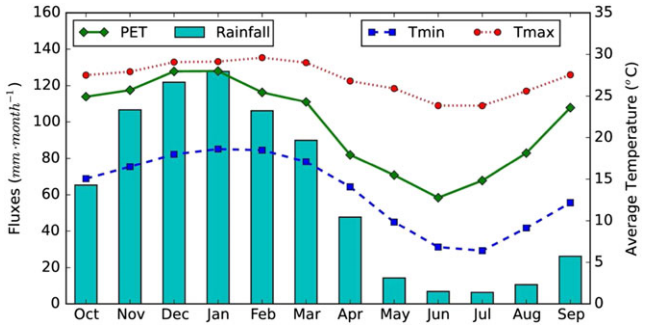

FIGURE 2 Long-term monthly average rainfall, potential evaporation, and minimum and maximum temperature for the Kaap catchment

was assumed to be similar to concentrations observed during rainfall events (Camacho Suarez, Saraiva Okello, Wenninger, & Uhlenbrook, 2015; van Wyk, van Tonder, & Vermeulen, 2011). The assumptions of this method are further discussed by Buttle (1994), Uhlenbrook et al. (2002), and Uhlenbrook and Hoeg (2003).

The two-component hydrograph separation was performed using EC. The main assumption for the definition of the groundwater end member is that during the dry season, the baseflow is essentially made up of groundwater alone. Thus, the highest percentiles of EC were considered to represent the groundwater signature.

The hydrograph separation was conducted using daily flow data and intermittent EC data; therefore, results are compared at monthly and annual scales.

2.4 | Digital filters hydrograph separation

Hydrograph separation using recursive digital filter approaches focus on distinguishing between rapidly occurring discharge components such as surface runoff and slowly changing discharge originating from interflow and groundwater (Rimmer & Hartmann, 2014).

The hydrograph separation algorithm for Equation 3 was implemented in Python code, to facilitate repetition, calibration, and plotting. The recursive digital filter (Eckhardt, 2005) is based on the

TABLE 2 Data used for rainfall, flow, and water quality

	Code	Name	Latitude	Longitude	Altitude	Start year	End year	Time resolution/number of samples	Institution/ source
Rainfall	0519733 9	Kamhlabane	−25.717	31.417	1205	1972	2014	Daily	SAWS
	0519518 7	Louws Creek-Pol	−25.633	31.300	477	1972	2014	Daily	SAWS
	0519168 0	Highlands	−25.800	31.100	1240	1995	2014	Daily	SAWS
	0519077 8	Barberton–TNK	−25.794	31.041	852	1972	2009	Daily	SAWS
	0518589 3	Nelshoogte Bos	−25.825	30.832	1400	1972	2014	Daily	SAWS
	0555750 9	Nelspruit	−25.500	30.916	883	1993	2014	Daily	SAWS
	0518393 3	Berlin Bos	−25.550	30.733	1341	1972	2014	Daily	SAWS
	0556088 4	Mayfern	−25.468	31.043	610	1973	2014	Daily	SAWS
	0518346 2	Onverwacht	−25.761	30.701	1403	1972	2014	Daily	SAWS
Flow	X2H008	Queens River at Sassenheim	−25.786	30.924		1948	2014	Daily	DWS–HS
	X2H010	North Kaap River at Bellevue	−25.611	30.875		1948	2014	Daily	DWS–HS
	X2H022	Kaap River at Dolton	−25.543	31.317		1960	2014	Daily	DWS–HS
	X2H031	South Kaap River at Bornmans drift	−25.730	30.978		1966	2014	Daily	DWS–HS
Water quality [a]	X2H008Q01	Queens River at Sassenheim	−25.786	30.924		1978	2012	465	DWS–WMS
	X2H010Q01	North Kaap River at Bellevue	−25.609	30.875		1978	2012	454	DWS–WMS
	X2H022Q01	Kaap River at Dolton	−25.542	31.317		1978	2012	940	DWS–WMS
	X2H031Q01	South Kaap River at Bornmans drift	−25.729	30.979		1978	2012	479	DWS–WMS

Note. DWS–HS = Department of Water and Sanitation (former Department of Water Affairs)–Hydrological Services, https://www.dwa.gov.za/hydrology/; DWS–WMS = Department of Water and Sanitation (former Department of Water Affairs)–Water Management System, https://www.dwa.gov.za/iwqs/wms/; SAWS = Southern Africa Weather Service.

[a]Water quality parameters include electrical conductivity, pH, calcium, magnesium, potassium, sodium, chloride, sulphates, total alkalinity, silica, fluoride, nitrates, ammonia, phosphate, and total dissolved salts.

assumption that the outflow from an aquifer is linearly proportional to its storage:

$$b_k = \frac{(1-BFI_{max})\alpha b_{k-1} + (1-\alpha)BFI_{max}y_k}{1-\alpha BFI_{max}}, \quad (3)$$

subject to $b_k \leq y_k$, where b_k is the baseflow flux on day k, y_k is total discharge on day k, α is the recession constant that is estimated from the recession limbs of the hydrograph, and BFI_{max} is the maximum value of the baseflow index (the long term ratio of baseflow to river discharge) that can be modelled by the algorithm.

According to Eckhardt (2005) and Eckhardt (2008), the BFI_{max} is a very sensitive parameter but is also nonmeasurable. Therefore, Eckhardt (2008) suggested that tracers can provide data for better calibration of BFI_{max}. The "BFI_{max}" parameter could be better defined using the independent results of tracer hydrograph separation (Cartwright et al., 2014; Rimmer & Hartmann, 2014; Zhang et al., 2013), which was the approach adopted in this research.

The parameter α was computed using three methods, described in Rimmer and Hartmann (2014): First, a master recession curve (Eckhardt, 2005) was constructed, where the daily streamflow data of several dry seasons were overlapped based on the day of the year (DOY) for the period of May to September (DOY 121–250). The master recession curve was created by averaging the flow during all seasons, and the exponent that best fitted the recession equation was used to compute α. Second, the correlation method (Tallaksen, 1995) was used, where α corresponds to the slope of the regression line through the origin in a scatter plot of streamflow Q_{j+1} against Q_j. Third, the mean value of Q_{j+1}/Q_j during the same dry period was calculated.

2.5 | Calibration of digital filter parameters with tracer data

The calibration procedure followed is based on Rimmer and Hartmann (2014) and Zhang et al. (2013). The end members of surface and baseflow were estimated from the EC data. The surface end member is fixed at 20 μS/cm, which corresponds to the average rainfall EC as reported by Camacho Suarez et al. (2015) and lowest observed EC from the stream. The baseflow end member was estimated from the highest observed EC in the streamflow. There is some uncertainty in literature on the best method to define this value, so a sensitivity analysis was conducted, assuming c_b would be the percentile 90, 95, 99, or max excluding outliers of the observed EC (Kronholm & Capel, 2015). The chemical hydrograph separation using EC was then performed, and a reference baseflow was estimated.

Digital filter (DF) separation using Eckhardt (2005) approach was conducted, with the α computed from recession analysis and initial estimate of BFI_{max} based on catchment geology (recommended 0.25 for perennial streams with hard rock aquifers). An optimization procedure was then used, whereby the time series of baseflow from the digital filter is compared with the tracer baseflow, goodness of fit indicators are computed, and an objective error function is minimized—that is, the root mean squared error (RMSE) between reference tracer baseflow and DF baseflow. The optimal BFI_{max}

parameter is the one that best fits tracer and DF methods, with minimal error, following the approach by (Rimmer & Hartmann, 2014). Both time series of baseflow were plotted for visual inspection, and goodness of fit indicators such as Nash–Sutcliffe (NS), RMSE, bias, and correlation coefficient were computed. Total baseflow indices are computed and compared as well.

All the analyses were conducted at daily time steps, subsequently being aggregated to monthly and annual timescale. However, calibration was conducted only for days were EC data were available.

3 | RESULTS

3.1 | Spatial and temporal variability of catchment hydrochemistry

The headwater catchments are characterized by waters with low EC (100 ± 25 μS/cm, average ± standard deviation), dominated by alkalinity. The range of EC at the outlet (120 to 1,200 μS/cm) is much higher than for the headwaters (40 to 400 μS/cm). The variation of EC at the outlet follows a marked cyclical pattern. EC increases in dry seasons up to 1,200 μS/cm and decreases during the wet season to 200 μS/cm, reflecting the relative flow volume in each season. The variation in the Noordkaap, for example, is much less accentuated with ranges between 50 to 200 μS/cm (Figure 3).

EC monthly variation is in the same range for the Queens (monthly average of 155 to 196 μS/cm), Noordkaap (monthly average of 98 to 123 μS/cm), and Suidkaap (monthly average of 133 to 182 μS/cm) tributaries. The EC is slightly higher in September (low flow) than in other months. Suidkaap, which is the tributary with the largest area and longest river length, exhibits more marked seasonality compared with the two smaller tributaries. The Kaap outlet shows a very strong seasonality of EC (monthly average of 405 to 711 μS/cm). There is also a pattern of higher EC in a sequence of dry years and lower values in wetter years.

The comparison of boxplots (Figure 4) reveals that EC, chloride, sodium, calcium, magnesium, sulphate, and total alkalinity are lower in the Noordkaap, followed by Suidkaap and Queens, and much higher in the Kaap; the Kaap outlet values are almost an order of magnitude higher than its contributing tributaries. For example, chloride ranges from 1.5 to 30.3 mg/L in the Noordkaap with average 4.8 ± 2.4 mg/L, whereas the range in the Kaap outlet is 3.7 to 57.2, with average 22.9 ± 9.7 mg/L. Silica, however, has a very similar range of values across the catchments. At the Kaap outlet, the mean concentration of silica (14.1 ± 3.0 mg/L) is only slightly higher than the tributaries (12.3 ± 2.2 mg/L), but the range of variation is much wider. Appendix A1 provides a table with detailed statistics of water quality for the Kaap catchment and its tributaries.

3.2 | Hydrograph separation

3.2.1 | Chemical hydrograph separation

In all hydrograph separations using EC, the important contribution of baseflow to total streamflow is evident. As expected, during the dry August and September months, the contribution of baseflow is relatively high, with baseflow index (BFI) of 0.82 ± 0.13 (average ± standard deviation). January and February have the lowest relative contribution with BFI 0.62 ± 0.17 in the Noodkaap tributary (Figure 5). In the Kaap outlet, the BFI in September is 0.81 ± 0.16 whereas the BFI in February is 0.48 ± 0.16.

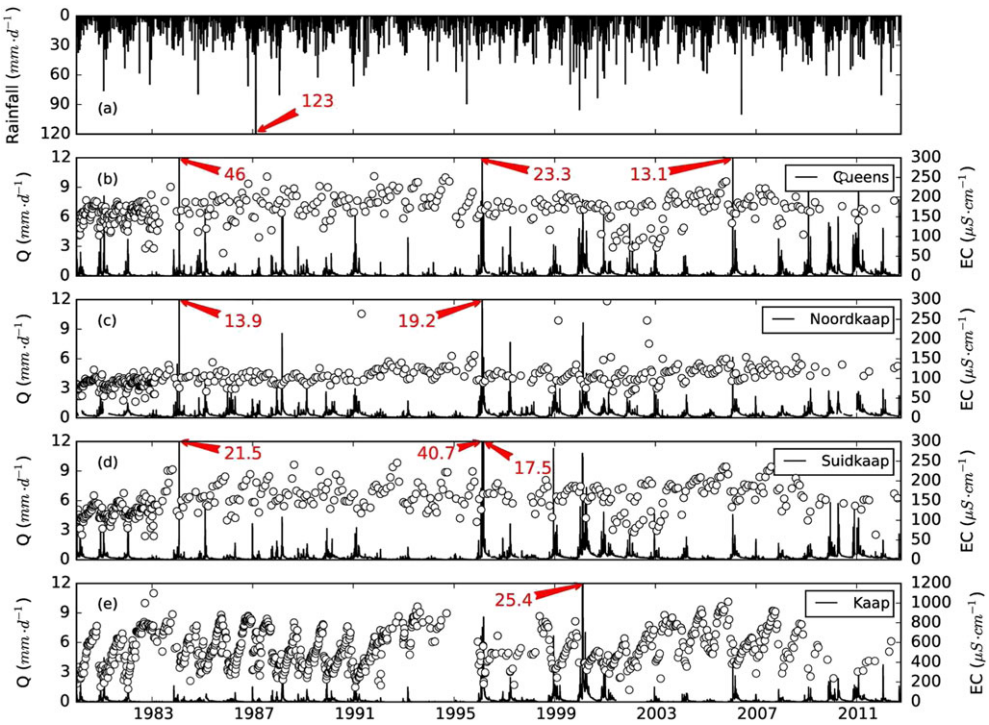

FIGURE 3 (a) Areal rainfall; flow (solid black line) and EC (circles) for (b) Queens, (c) Noordkaap, (d) Suidkaap, and (e) Kaap catchments; 1978–2012. Red arrows indicate rainfall and flow values higher than y-axis

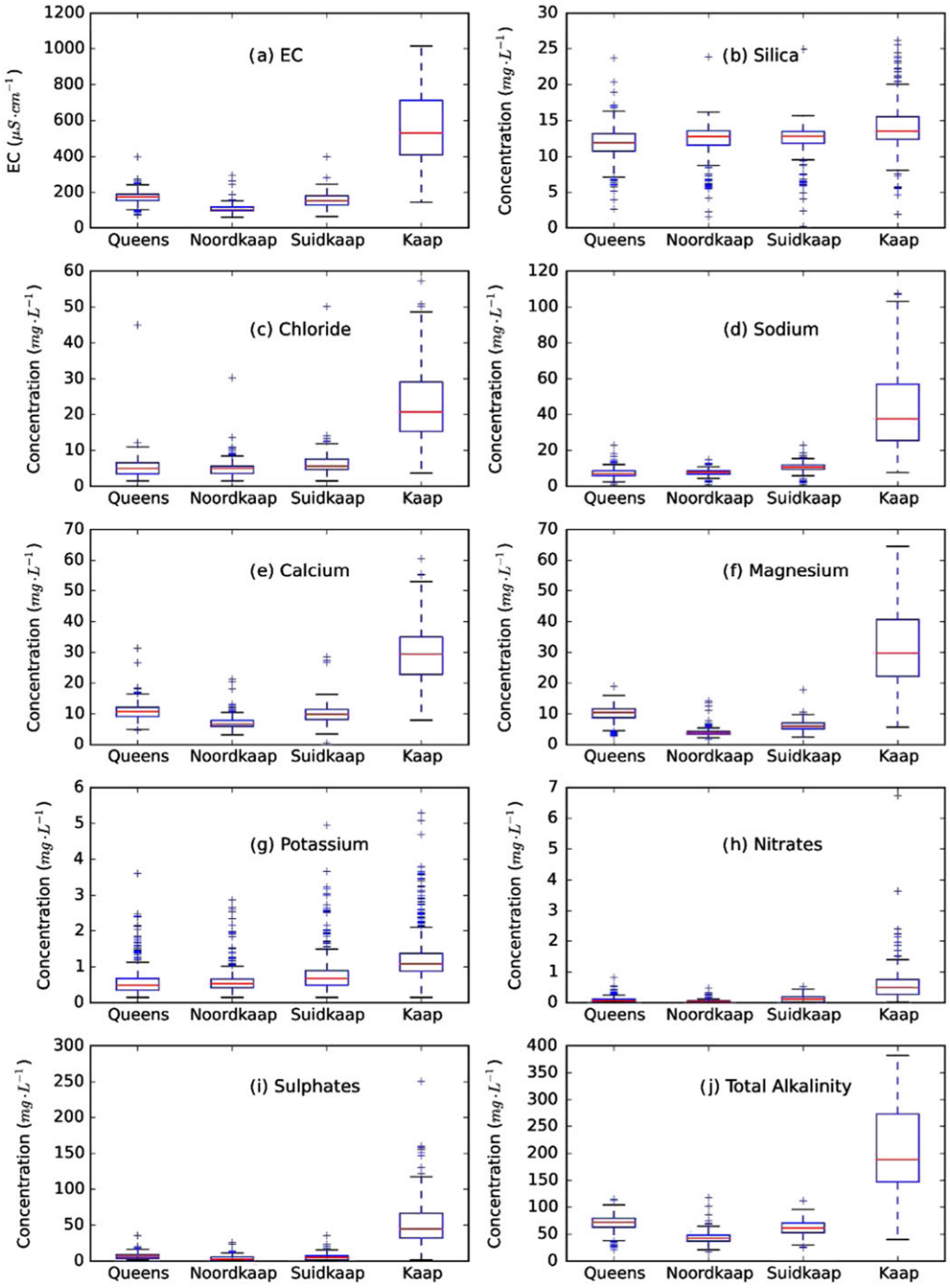

FIGURE 4 Comparison of boxplots of water quality for the four catchments: (a) EC, (b) silica, (c) chloride, (d) sodium, (e) calcium, (f) magnesium, (g) potassium, (h) nitrates, (i) sulphate, (j) total alkalinity

3.2.2 | Hydrograph separation using digital filters

The hydrograph separation using digital filters was conducted within the calibration and optimization routine in python. The parameter α was calculated from master recession curve analysis for each catchment, using three methods (Rimmer & Hartmann, 2014). Figure 6 illustrates the calculation of α using the correlation method. The value of α was then fixed as the average of the three methods, as presented on Table 3.

The parameter BFI_{max} was initially estimated as BFI_{max} = 0.25 for perennial rivers dominated by hard rock aquifer (Eckhardt, 2005). This parameter was then optimized to better fit the estimated baseflow from digital filter to the reference tracer baseflow. Table 4 presents the results of optimized BFI_{max}, the c_s and c_b used, and the goodness of fit indicators, as well as total baseflow from tracer and digital filter separation methods.

3.3 | Calibration of digital filter using tracers and sensitivity analysis

Figure 7 shows the results of the calibration exercise (conducted for the entire time series) for the four catchments for the period 1997 to 2005.

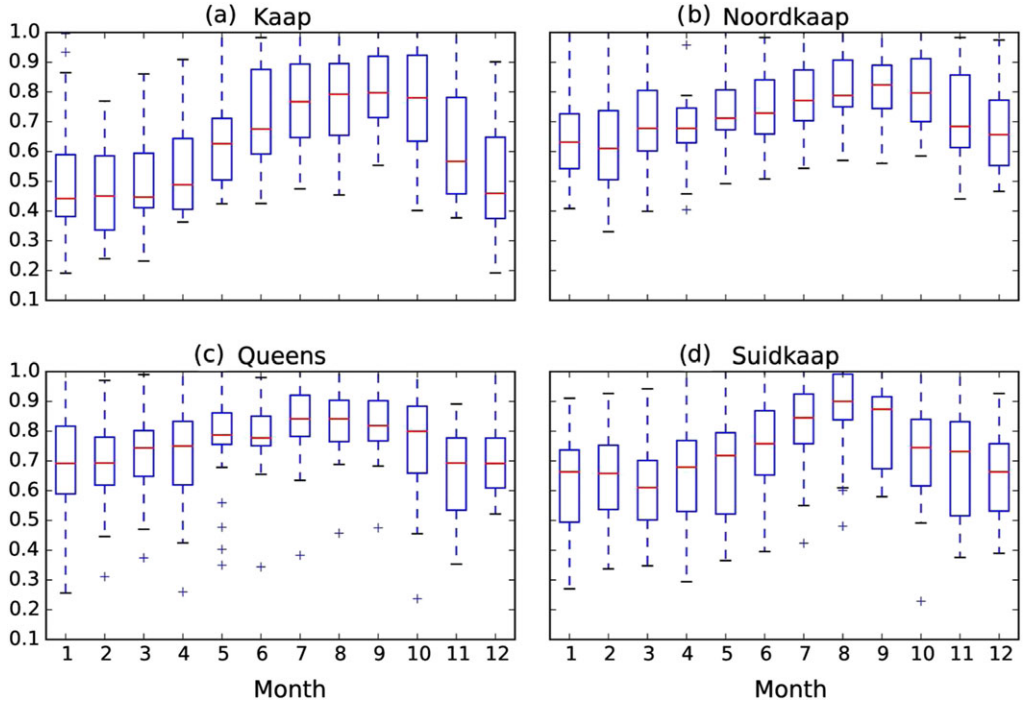

FIGURE 5 Boxplots of baseflow index (nondimensional) derived from chemical hydrograph separation per month, for the period of 1978 to 2011: (a) Kaap, (b) Noordkaap, (c) Queens, and (d) Suidkaap. For this separation, the groundwater end member was defined as 95% percentile of EC time series. Month 1 corresponds to January and 12 to December

The digital filter fills the gaps where tracer data are not available, and it is possible that it overestimates the peaks, given that less tracer data are available during peaks compared with normal or low flow. In some occasions, the digital filter also seems to underestimate or overestimate the low flows, particularly at Suidkaap and Queens. However, it is evident that the variability of the hydrograph is generally well captured by the calibrated digital filter results.

Overall, good to very good correlations were achieved between reference tracer separation and the calibrated digital filter. Correlation coefficient ranged from 0.753 to 0.961 for all the calibrations. The NS coefficient ranged from 0.375 to 0.91 with RMSE ranging from 0.10 to 0.29 (Table 4).

The optimal BFI_{max} for the Noordkaap catchment ranged from 0.482 (99% used for c_b) to 0.744 (90% for c_b), which corresponded to total baseflow of 48% to 68%, respectively. The correlation between digital filter baseflow and reference tracer baseflow ranged from 0.753 to 0.842, which shows a good correlation between them. The difference between total baseflow from calibrated DF and tracer was minimal. The RMSE ranged from 0.123 to 0.145.

The Queens catchment however showed some distinct results. The tracer separation suggested high baseflow contributions, resulting in even higher baseflow contributions for the calibrated DF separation. Optimal BFI_{max} ranged from 0.935 to 0.964, with very high correlation coefficients (0.925 to 0.961). Using the tracer method, total baseflow was 55 to 70%, whereas for the calibrated filter, it was 78% to 84%. This resulted in a difference of 21% to 42%. The RMSE ranged from 0.236 to 0.29, whereas the NS varied from 0.817 to 0.91.

The Kaap outlet had the lowest $BFI_{max,}$ ranging from 0.271 to 0.50, which yielded a total baseflow of 26% to 45% using the calibrated filter. RMSE were the lowest, ranging from 0.10 to 0.133, whereas NS were also the lowest (0.375 to 0.653).

3.4 | Runoff components

3.4.1 | Monthly scale

The results of digital filter hydrograph separation with calibrated parameters using c_b of 95% percentile were aggregated to monthly volumes. Figure 8 illustrates the average monthly flow components for the catchments, and Appendix A2 presents more detailed results of both monthly and annual flow components. The variability of flow components in a monthly scale is high, due to the high variability of rainfall and thus flow. Highest baseflow and quickflow volume contributions occur in February and March.

In the Queens catchment, the baseflow component ranges from $0.32 \cdot 10^6 \pm 0.3 \cdot 10^6$ m^3 (average ± standard deviation) in August to $2.28 \cdot 10^6 \pm 2.61 \cdot 10^6$ m^3 in February. The average monthly quickflow is highest in January ($0.76 \cdot 10^6 \pm 1.2 \cdot 10^6$ m^3) and lowest in August ($0.02 \cdot 10^6 \pm 0.02 \cdot 10^6$ m^3). The highest baseflow ($11.5 \cdot 10^6$ m^3) occurred in the flood of February 1996. Highest quickflow ($6.2 \cdot 10^6$ m^3) however occurred during the flood of January of 1984.

The Noordkaap catchment exhibits a similar pattern but with highest average monthly baseflow in March ($1.47 \cdot 10^6 \pm 0.99 \cdot 10^6$ m^3) and lowest in October ($0.44 \cdot 10^6 \pm 0.2 \cdot 10^6$ m^3). The quickflow ranges from $0.13 \cdot 10^6 \pm 0.07 \cdot 10^6$ m^3 in June to $1.24 \cdot 10^6 \pm 1.65 \cdot 10^6$ m^3 in February. In this catchment, the peak baseflow occurred in March 1996 ($4.53 \cdot 10^6$ m^3) and highest quickflow during the flood of February 2000 ($7.4 \cdot 10^6$ m^3).

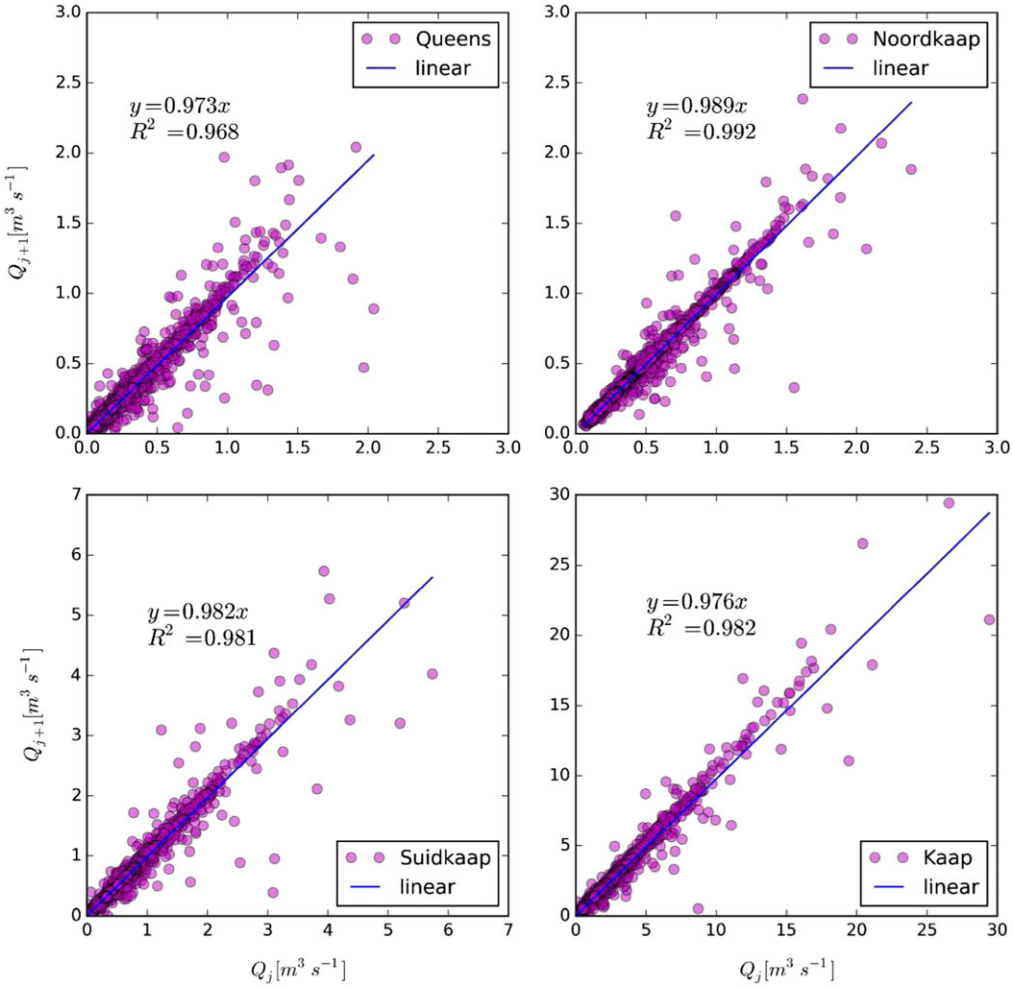

FIGURE 6 Calculation of α parameter using the correlation method (second method), for the four investigated catchments: (a) Queens, (b) Noordkaap, (c) Suidkaap, and (d) Kaap. α corresponds to the slope of the regression line through the origin in a scatterplot of streamflow Q_{j+1} against Q_j

TABLE 3 Results of computation of parameter α using the three methods suggested by Rimmer and Hartmann (2014)

	Method 1	Method 2	Method 3	Average
	Master recession curve exponent	Slope of regression of Q_{j+1} vs. Q_j	Mean of Q_{j+1}/Q_j	
Queens	0.989	0.973	0.988	0.98
Noordkaap	0.995	0.989	0.993	0.99
Suidkaap	0.995	0.982	0.992	0.99
Kaap	0.985	0.976	0.983	0.98

In the Suidkaap catchment, the baseflow component ranges from $0.69 \cdot 10^6 \pm 0.49 \cdot 10^6$ m^3 in October to $2.28 \cdot 10^6 \pm 2.1 \cdot 10^6$ m^3 in March. The average monthly quickflow is highest in February ($2.1 \cdot 10^6 \pm 3.88 \cdot 10^6$ m^3) and lowest in June ($0.22 \cdot 10^6 \pm 0.13 \cdot 10^6$ m^3). Similar to the other catchments, the peaks of baseflow ($10.2 \cdot 10^6$ m^3) and quickflow ($19.7 \cdot 10^6$ m^3) occured during the floods of 2000 and 1996.

In the Kaap catchment, the monthly average baseflow component ranges from $0.77 \cdot 10^6 \pm 0.87 \cdot 10^6$ m^3 in October to $7.34 \cdot 10^6 \pm 11.33 \cdot 10^6$ m^3 in March. The average quickflow is highest in February ($16.1 \cdot 10^6 \pm 37.0 \cdot 10^6$ m^3) and lowest in August ($0.84 \cdot 10^6 \pm 0.91 \cdot 10^6$ m^3). For the Kaap, the peak baseflow occurred in March 2000 ($54.5 \cdot 10^6$ m^3) and highest quickflow during the flood of February 2000 ($193.7 \cdot 10^6$ m^3). In this catchment, there are several months with minimum flow, baseflow, and quickflow of zero, occurring during the drought of 1992–1994.

3.4.2 | Annual scale

In Figure 9, the results of digital filter separations are aggregated to hydrological year total volumes for the entire analysis period

TABLE 4 Results of calibration of digital filter parameters with chemical hydrograph separation, using EC

Catchment	Percentile C_b	α	BFI_{max}	C_s	C_b	Correl	RMSE	NS	BFI_tr	BFI_DF	Difference, %
Noordkaap	90	0.99	0.744	20	128	0.842	0.145	0.689	67.9	68.5	1
	95	0.99	0.652	20	138	0.816	0.140	0.628	62.5	61.7	−1
	99	0.99	0.482	20	172	0.753	0.123	0.436	48.8	47.3	−3
	Max[a]	0.99	0.568	20	154	0.787	0.132	0.556	55.3	55.0	−1
Suidkaap	90	0.99	0.793	20	194	0.871	0.280	0.731	64.8	66.2	2
	95	0.99	0.692	20	210	0.843	0.279	0.672	59.5	60.2	1
	99	0.99	0.637	20	236	0.828	0.275	0.647	52.5	56.7	8
	Max[a]	0.99	0.539	20	246	0.787	0.267	0.540	50.2	50.1	0
Queens	90	0.98	0.964	20	205	0.961	0.236	0.910	69.8	84.2	21
	95	0.98	0.955	20	222	0.950	0.256	0.881	64.0	82.0	28
	99	0.98	0.935	20	255	0.925	0.290	0.817	55.1	78.0	42
	Max[a]	0.98	0.942	20	242	0.934	0.278	0.842	58.3	79.4	36
Kaap outlet	90	0.98	0.500	20	784	0.821	0.133	0.653	44.3	44.8	1
	95	0.98	0.412	20	833	0.791	0.128	0.556	41.7	38.3	−8
	99	0.98	0.341	20	921	0.773	0.118	0.468	37.6	32.6	−13
	Max[a]	0.98	0.271	20	1100	0.757	0.101	0.375	31.4	26.3	−16

Note. C_b is the EC concentration of groundwater end member (μS/cm), C_s is the EC surface water end member (μS/cm), α and BFI_{max} are digital filter parameters, Correl, RMSE and NS are indicators of goodness of fit. BFI_Tr is total baseflow (%) using chemical hydrograph separation BFI_DF is total baseflow (%) using digital filter, and their difference.

[a]Maximum EC excluding outliers.

(1978–2012). At the annual scale, it is evident that in drier years, most of the flow is composed of baseflow, whereas in wetter years, the baseflow contribution is close to the BFI_{max} percentage (40% to 70%).

In the Queens catchment, the baseflow contribution ranges from $1.4 \cdot 10^6$ to $42.3 \cdot 10^6$ m^3/y. The lowest contribution occurred during the drought of 1992–1994 and in 1983, whereas the highest occurred in 2000 and 2011. The annual average baseflow is about $13.7 \cdot 10^6$ m^3/y, which corresponds to about 82% of the total flow. The quickflow ranges from $0.4 \cdot 10^6$ to $8.1 \cdot 10^6$ m^3/y, with average of $3.0 \cdot 10^6$ m^3/y, corresponding to a 0.23 ratio of quickflow to baseflow.

The Noordkaap has a lower range of baseflow, varying from $2.9 \cdot 10^6$ to $24.5 \cdot 10^6$ m^3/y. The annual average baseflow is $10.3 \cdot 10^6$ m^3/y, constituting 62% of total flow. The quickflow ranges from $2.0 \cdot 10^6$ to $15.7 \cdot 10^6$ m^3/y, with average $6.4 \cdot 10^6$ m^3/y, corresponding to 0.62 quickflow to baseflow ratio.

The total baseflow contribution in the Suidkaap is about 60% of total flow, with average baseflow of $16.4 \cdot 10^6$ m^3/y. The average quickflow contribution is $10.9 \cdot 10^6$ m^3/y, which corresponds to 0.66 ratio of quickflow to baseflow. During the analysis period (hydrological years of 1978 to 2012), the baseflow ranged from $3.2 \cdot 10^6$ to $56.7 \cdot 10^6$ m^3/y and quickflow from $2.4 \cdot 10^6$ to $38.0 \cdot 10^6$ m^3/y.

At the Kaap outlet, the range of variation of baseflow is the widest, with a minimum of $0.3 \cdot 10^6$ to a maximum of $237.9 \cdot 10^6$ m^3/y. The Kaap also had the highest contributions from quickflow, ranging from $1.2 \cdot 10^6$ to $358.5 \cdot 10^6$ m^3/y, with average $63.4 \cdot 10^6$ m^3/y. Similar to the other catchments, the minimum baseflow occurred in the drought of 1994 and the maximum in the wet year 2000. The average baseflow at the outlet is $39.4 \cdot 10^6$ m^3/y and total baseflow contribution is about 38% of total flow. The quickflow to baseflow ratio is 1.61, which is the highest of all catchments, highlighting the importance of quickflow in the Kaap river valley.

4 | DISCUSSION

4.1 | Hydrochemical analysis and applicability of tracers for hydrograph separation

The analysis of water quality data revealed that EC was a suitable tracer to perform hydrograph separation for the Kaap catchment. This is in line with several authors who have used high frequency and discrete time series of EC to perform hydrograph separation and quantify baseflow at a daily timescale (Longobardi et al., 2016; Miller et al., 2014; Miller et al., 2015; Zhang et al., 2013). For example, Miller et al. (2015) used discrete EC data sets to quantify baseflow contributions in the Upper Colorado basin, using hydrograph separation. They were able to quantify this component of the water budget, in a very heavily regulated and snowmelt dominated catchment. Hughes et al. (2003) used recursive digital filters to derive baseflow at monthly timescale for catchments in South Africa. They were able to derive baseflow parameters for use in the Pitman model, which is widely used for water resources assessment in South Africa. Li et al. (2014) estimated baseflow and groundwater recharge based on a similar approach of EC and recursive digital filter for a small watershed in Canada.

The high variability of water quality parameters including EC constitutes an important challenge to the end member definition of chemical hydrograph separation, as already noted by many authors (Miller et al., 2014). This makes the quantification of runoff components at various timescales rather indicative than exact; however, the temporal course and behaviour reveals relevant insights into the dynamics of the system.

EC is strongly correlated with other hydrochemical parameters, such as calcium, magnesium, and chloride (see Appendix A1 for multivariate analysis of water quality parameters). Most hydrochemical parameters exhibit a pattern of dilution during the wet season (October to March) and concentration in the dry season (April to September); this is likely due to high evaporation rates, lower flow

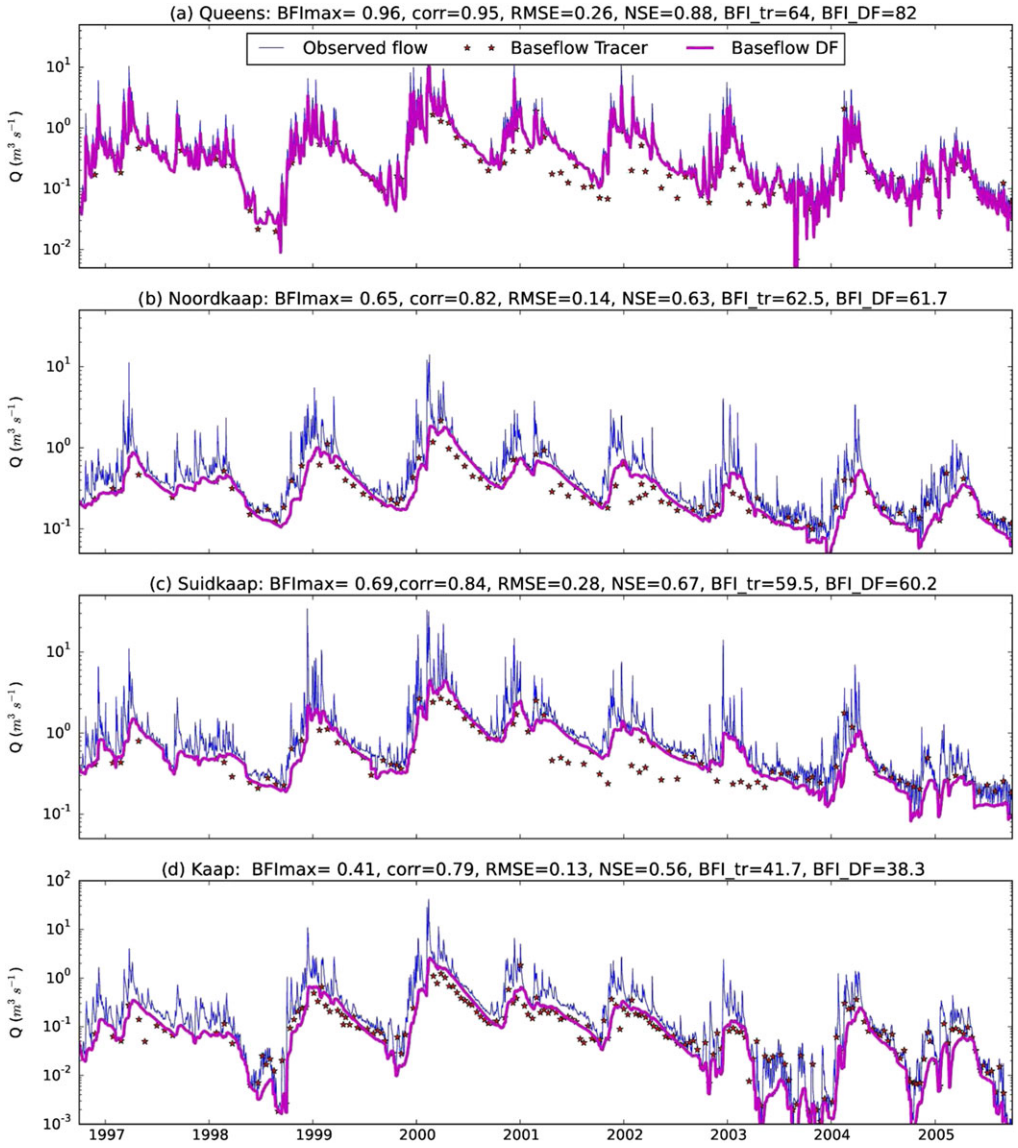

FIGURE 7 Results of calibration of the digital filter with tracers, for the period 1997–2005 (hydrological years) for the four investigated catchments: (a) Queens, (b) Noordkaap, (c) Suidkaap, and (d) Kaap. Baseflow DF is the baseflow resulting from digital filter separation and baseflow tracer is the baseflow estimated from chemical hydrograph separation

available during the dry season, and relative stronger contributions from groundwater sources and possible anthropogenic sources (irrigation return flow and wastewater). Some studies in South Africa, for example, Sahula (2014), also report that increased urbanization and informal settlements contribute with both point and nonpoint pollution, due to discharges from untreated sewage. In the Kaap catchment, this is combined with abandoned mines and irrigation return flows thereby impacting the water quality in the river significantly (Deksissa, Ashton, & Vanrolleghem, 2003; Retief, 2014; Sahula, 2014; Slaughter & Hughes, 2013).

EC increases dramatically after the confluence of the Noordkaap and Suidkaap River. This is also the section where there is a major change in geology, topography, and land use. Furthermore, the land use includes some industries, mining, and irrigated agriculture, which will likely increase the load that contributes to EC through effluents and return flows (Deksissa et al., 2003; Retief, 2014). The input of return flows were not taken into account for the two-component hydrograph separation, given that not enough information is available regarding the timing, volume, and load of these. Further research is required to quantitatively assess which factor could be the most important cause of this EC increase.

4.2 | Derivation and validity of results obtained by digital filters

Digital filters are very useful and inexpensive to quantify baseflow contributions. Recursive digital filters in particular are the most developed method to perform hydrograph separation using the streamflow records alone (Eckhardt, 2008).

However, given the high sensitivity of the digital filter parameters, it is important that calibration of parameters is done prior to operational use of baseflow estimates. When water quality data are available through routine sampling campaigns, or dedicated experiments, it can be used to calibrate digital filters. It is recommended that high frequency water quality data are used in a number of sites in the catchment to perform the calibration of digital filters (Longobardi

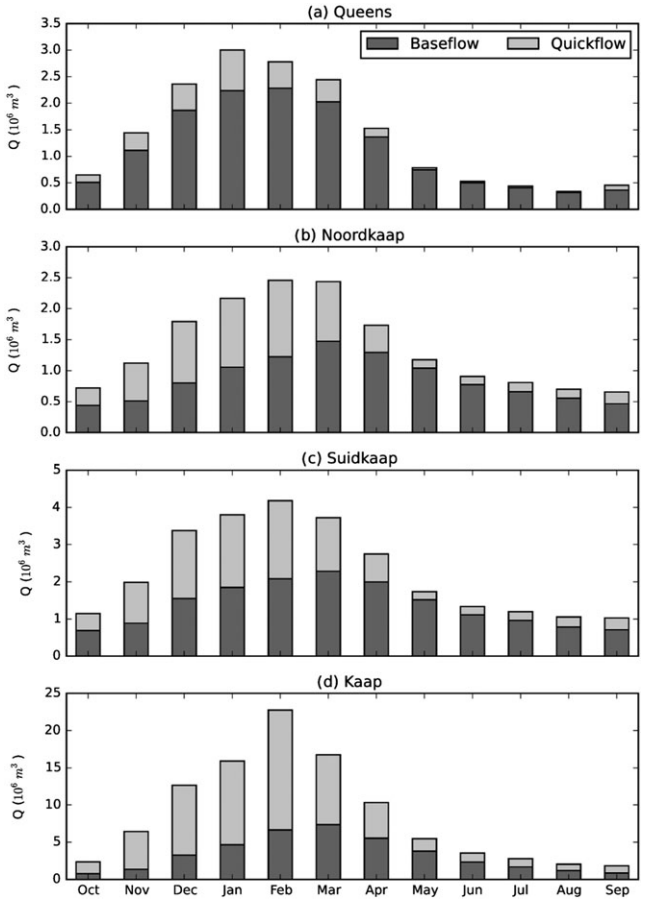

FIGURE 8 Monthly average flow components using calibrated digital filters: (a) Queens, (b) Noordkaap, (c) Suidkaap, and (d) Kaap

et al., 2016; Zhang et al., 2013). Once the filter parameters are calibrated, the entire flow time series can be used to derive a similar time series of baseflow, such as in the study of Zhang et al. (2013).

The parameter α, for example, can be determined by recession curve analysis (Table 3). The parameter BFI_{max} requires more calibration, as it is more sensitive than α, and cannot be physically measured (Eckhardt, 2005; Eckhardt, 2012; Rimmer & Hartmann, 2014). In this study, we found that once α is determined, BFI_{max} can be optimized to fit observed time series of EC. BFI_{max} is more sensitive to the baseflow end member of EC. Thus, for the sensitivity analysis, we looked at 90%, 95%, and 99% percentiles of EC for c_b definition. For 90 and 95, the results are quite similar and comparable, but when 99% c_b is used, the BFI_{max} is much smaller than with other percentiles. This finding is critical, because the 99% c_b could include some EC outliers that greatly bias the separation. Therefore, the 95% was adopted for this study as reference end member for c_b.

This study demonstrates that data collected by routine campaigns (weekly/monthly) can be useful for calibration of digital filters, similar to the studies of Rimmer and Hartmann (2014) and Li et al. (2014). The calibration data can be discrete but with greater temporal resolution this improves, as the definition of end members is based on a more informative data set (covering a range of flow/EC relationships). Additionally, we found that the calibrated BFI_{max} is, in most cases, higher than the BFI_{max} values found in the literature for perennial rivers with predominant hard rock aquifers (Eckhardt, 2005).

4.3 | Implications for hydrological process understanding

This study revealed the importance of seasonality on the flow generation in the Kaap catchment. Baseflow is a very important component of river flow, particularly during the dry season (May–September). During the wet season (October–March), baseflow still contributes about 40% to 60% of river flow. Hughes et al. (2003) also reported very high baseflow contribution of over 60% in a tributary of the nearby Sabie River.

In the Kaap River, however, the volumetric baseflow contribution appears to be lower than in other subcatchments. Camacho Suarez et al. (2015) conducted an intense tracer study in the Kaap catchment during the wet season of 2013/2014. They used both hydrochemical and environmental tracers and reported groundwater contribution of 64% to 98% in four events studied, based on daily and shorter timescale data. This seems to contradict the digital filter results, but a lot of water abstractions (mainly surface water) occur on the lower Kaap valley. Mallory and Beater (2009) report a crop water requirement of $91.7 \cdot 10^6$ m^3/y, for about 98 km^2 of sugarcane irrigation. They further report that $62 \cdot 10^6$ m^3/y is supplied to the irrigation boards—this is about 33% of the naturalized mean annual runoff of $189 \cdot 10^6$ m^3/y (Bailey & Pitman, 2015). Most of the water is abstracted from the river flow during the dry months, which explains the apparent low baseflow contributions in the Kaap catchment. In the wet season, the water demand for irrigation is reduced; therefore, the quickflows are not greatly affected.

Furthermore, Saraiva Okello et al. (2015) studied the drivers of streamflow variability in the Incomati Basin (where the Kaap catchment is a tertiary subcatchment). They found that plantations (eucalyptus and pine) and irrigation caused a significant decline on streamflow in several streamflow gauges in the Crocodile catchment, including the Noordkaap and Kaap. About $39.8 \cdot 10^6$ m^3/y is attributed to afforestation in the Kaap catchment (Mallory & Beater, 2009), which is considered a streamflow reduction activity in South Africa. This finding was also supported by van Eekelen et al. (2015), in a study were remote sensing was used to estimate direct and indirect water withdrawals in the Incomati basin.

4.4 | Application in water resources management

The flow components information is important for the understanding and quantification of environmental flows, as well as to better parameterize the hydrological models used for water resources planning and management, particularly rainfall–runoff models (O'Brien, Misstear, Gill, Johnston, & Flynn, 2014).

Another finding of this study is that the simple model of two-component mixing can work relatively well at smaller headwater catchments (such as the Noordkaap in this study), but it is not sufficiently complex to characterize the runoff generation processes that occur at a mesoscale catchment (such as the Kaap). This can also be explained by the fact that the headwater catchments often have a more homogenous geology and land use, but in a larger catchment, the heterogeneity of geology, soils, and land use increases as well as human influence can introduce new components, for instance, return

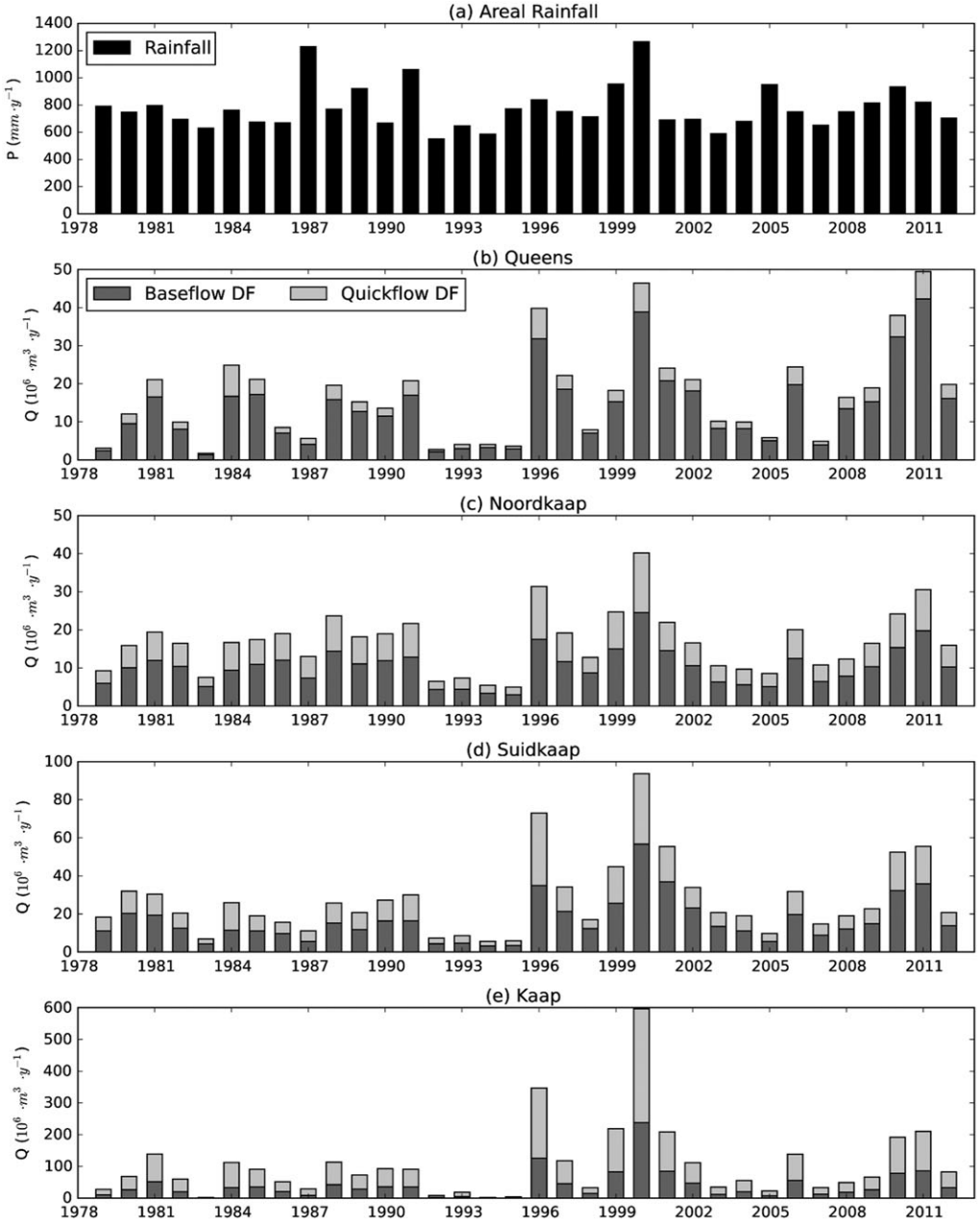

FIGURE 9 Summary of hydrograph separation using calibrated digital filters, 1978–2012: (a) areal rainfall, (b) Queens, (c) Noordkaap, (d) Suidkaap, and (e) Kaap. The rainfall and hydrograph is aggregated by hydrological year total volumes. Note the different vertical scales

flows from irrigated agriculture. For the larger catchment, more intense monitoring is required to account for different flow contributions and anthropogenic activities.

This research further highlights that even though the chemical hydrograph separation is a useful concept, it is quite difficult to determine the exact values of end member components at mesoscale catchments. In fact, these end members are not physically observed and measured in one spot but are the result of an assumed mixing of various sources in a complex reality. The rainfall input, for example, is distributed over a large catchment area and interacts with the land surface, soils, and stagnant water before it reaches the river and becomes streamflow. The amount of rainfall that falls directly on the river course is insignificant compared with the amount that is routed as surface runoff during intense rainfall events. Therefore, even though we assume that this component resembles rainfall water quality, it is likely to have a much more diverse water quality signature.

The baseflow, on the other hand, is also composed of components from different sources. Baseflow, which is the flow that feeds the river during extended periods without rainfall, can be composed of deep regional groundwater discharge, localized shallow groundwater, return flows from irrigated agriculture, discharge from municipal water use, discharge from informal settlements, or releases from reservoirs, among others.

The use of calibrated digital filters still reveals important insights of the catchment flow dynamics at daily, monthly and annual scales, which are useful for quantification of environmental flows, river operation, and conjunctive groundwater management.

5 | CONCLUDING REMARKS

In this study, we analysed historical hydrochemical data and used it to perform two-component hydrograph separations at monthly and annual timescale in a mesoscale semi-arid catchment and three subcatchments. There is strong seasonality in the runoff and hydrochemistry in all catchments, particularly at the main outlet.

Electrical conductivity was identified as a suitable tracer to perform chemical hydrograph separation for these catchments, given the consistency of the data set. The chemical hydrograph separation indicates that the baseflow dominates the total flow, with contributions ranging from 50% in wet season to 90% in dry season.

Hydrograph separation was also performed using Eckhardt's recursive digital filter, with daily streamflow data. The parameter BFI_{max} was calibrated for different sets of groundwater end members, using the chemical hydrograph separation for reference.

The digital filter parameters are very sensitive, and their use without calibration is not recommended, as they can yield very different quantitative results. Optimal sets of α and BFI_{max} were identified for the studied catchments. In spite of the uncertainties in α and BFI_{max}, the digital filter hydrograph separation is very useful to interpolate and to extend baseflow estimates for periods where tracer data are not available. It is recommended that more calibration studies are conducted in semi-arid catchments to assess if regionalization (transfer in space) of filter parameters is possible.

Another important finding of this study is the high contribution of baseflow to total flow during both wet and dry conditions. This means that the groundwater reservoirs respond quickly during storm events, which is important to consider for flood forecasting, environmental flow assessments, and for land use planning and management, in order to optimize/enhance groundwater recharge or prevent practices that compromise this.

This study has tested the usefulness of using readily available secondary water quality data to calibrate hydrograph separation using recursive digital filters. We also tested a method to optimize the BFI_{max} parameter used in digital filter methods for hydrograph separation. Once the parameters for the digital filter separation are calibrated, it is possible to perform hydrograph separation for much more extensive periods of time than the available water quality data. Also, the digital filter performs separation in a daily basis, whereas water quality data are only available at weekly or monthly time steps. So a more refined separation is possible using this approach.

The relevance of this analysis is that it allows for estimation of the baseflow component on a daily basis, from readily available streamflow and water quality data. Thus, these findings can be used to improve rainfall–runoff models, especially in terms of conjunctive groundwater management, river operations, and quantification of environmental flows where decisions regarding releases from dams and/or abstractions from rivers are done on a daily/weekly basis.

ACKNOWLEDGMENTS

The authors would like to thank the RISKOMAN (Risk-based operational water management for the Incomati River Basin) project partners for financial support and data provided. We appreciate the financial support of the Water Research Commission of South Africa, through project K5/1935. We particularly thank the Department of Water and Sanitation and the Inkomati-Usuthu Catchment Management Agency for hydrometric and water quality data provided. We thank the South African Weather Service for climatic data provided. The financial contribution through research grants from L'Oreal-UNESCO "For Women in Science, Sub-Saharan Africa 2013" and Schlumberger Foundation "Faculty of the Future Fellowship 2014-2015" to the first author is highly appreciated. The constructive comments of anonymous reviewers and associate editor are greatly appreciated.

ORCID

Aline Maraci Lopes Saraiva Okello http://orcid.org/0000-0002-2851-3372

Pieter Van der Zaag http://orcid.org/0000-0002-1215-2656

REFERENCES

Bailey, A., & Pitman, W. (2015). Water resources of South Africa, 2012 study: User guide. Water Research Comission.

Beven, K. J. (2012). *Rainfall-runoff modelling: The primer*. Chichester, England: John Wiley & Sons.

Birkel, C., Soulsby, C., & Tetzlaff, D. (2014). Developing a consistent process-based conceptualization of catchment functioning using measurements of internal state variables. *Water Resources Research*, *50*, 3481–3501. https://doi.org/10.1002/2013wr014925

Birkel, C., Tetzlaff, D., Dunn, S. M., & Soulsby, C. (2010). Towards a simple dynamic process conceptualization in rainfall–runoff models using multi-criteria calibration and tracers in temperate, upland catchments. *Hydrological Processes*, *24*, 260–275. https://doi.org/10.1002/hyp.7478.

Blöschl, G., Sivapalan, M., Wagener, T., Viglione, A., & Savenije, H. (2013). *Runoff prediction in ungauged basins: Synthesis across processes, places and scales*. Cambridge, U. K: Cambridge University Press.

Buttle, J. M. (1994). Isotope hydrograph separations and rapid delivery of pre-event water from drainage basins. *Progress in Physical Geography*, *18*, 16–41. https://doi.org/10.1177/030913339401800102

Camacho Suarez, V. V., Saraiva Okello, A. M. L., Wenninger, J. W., & Uhlenbrook, S. (2015). Understanding runoff processes in a semi-arid environment through isotope and hydrochemical hydrograph separations. *Hydrology and Earth System Sciences*, *19*, 4183–4199. https://doi.org/10.5194/hess-19-4183-2015

Capell, R., Tetzlaff, D., Malcolm, I. A., Hartley, A. J., & Soulsby, C. (2011). Using hydrochemical tracers to conceptualise hydrological function in a larger scale catchment draining contrasting geologic provinces. *Journal of Hydrology*, *408*, 164–177. https://doi.org/10.1016/j.jhydrol.2011.07.034.

Capell, R., Tetzlaff, D., & Soulsby, C. (2012). Can time domain and source area tracers reduce uncertainty in rainfall-runoff models in larger heterogeneous catchments? *Water Resources Research*, *48*, W09544. https://doi.org/10.1029/2011wr011543

Cartwright, I., Gilfedder, B., & Hofmann, H. (2014). Contrasts between estimates of baseflow help discern multiple sources of water contributing to rivers. *Hydrology and Earth System Sciences*, *18*, 15–30. https://doi.org/10.5194/hess-18-15-2014

de Wit, M. J., Furnes, H., & Robins, B. (2011). Geology and tectonostratigraphy of the Onverwacht suite, Barberton Greenstone Belt, South Africa. *Precambrian Research*, *186*, 1–27. https://doi.org/10.1016/j.precamres.2010.12.007.

Deksissa, T., Ashton, P. J., & Vanrolleghem, P. A. (2003). Control options for river water quality improvement: A case study of TDS and inorganic nitrogen in the Crocodile River (South Africa). *Water SA*, *29*, 209–218.

Eckhardt, K. (2005). How to construct recursive digital filters for baseflow separation. *Hydrological Processes*, *19*, 507–515. https://doi.org/10.1002/hyp.5675

Eckhardt, K. (2008). A comparison of baseflow indices, which were calculated with seven different baseflow separation methods. *Journal of Hydrology*, *352*, 168–173. https://doi.org/10.1016/j.jhydrol.2008.01.005.

Eckhardt, K. (2012). Technical note: Analytical sensitivity analysis of a two parameter recursive digital baseflow separation filter. *Hydrology and Earth System Sciences*, *16*, 451–455. https://doi.org/10.5194/hess-16-451-2012

Frisbee, M. D., Phillips, F. M., White, A. F., Campbell, A. R., & Liu, F. (2013). Effect of source integration on the geochemical fluxes from springs. *Applied Geochemistry*, *28*, 32–54. https://doi.org/10.1016/j.apgeochem.2012.08.028.

Gonzales, A. L., Nonner, J., Heijkers, J., & Uhlenbrook, S. (2009). Comparison of different base flow separation methods in a lowland catchment. *Hydrology and Earth System Sciences*, *13*, 2055–2068. https://doi.org/10.5194/hess-13-2055-2009

Hall, F. R. (1968). Base-flow recessions—A review. *Water Resources Research*, *4*, 973–983. https://doi.org/10.1029/WR004i005p00973

Hengl, T., de Jesus, J. M., MacMillan, R. A., Batjes, N. H., Heuvelink, G. B., Ribeiro, E., … Walsh, M. G. (2014). SoilGrids1km—Global soil information based on automated mapping. *PLoS One*, *9*, e105992.

Hengl, T., Mendes de Jesus, J., Heuvelink, G. B. M., Ruiperez Gonzalez, M., Kilibarda, M., Blagotić, A., … Kempen, B. (2017). SoilGrids250m: Global gridded soil information based on machine learning. *PLoS One*, *12*, e0169748. https://doi.org/10.1371/journal.pone.0169748

Hessler, A. M., & Lowe, D. R. (2006). Weathering and sediment generation in the Archean: An integrated study of the evolution of siliciclastic sedimentary rocks of the 3.2 Ga Moodies group, Barberton Greenstone Belt, South Africa. *Precambrian Research*, *151*, 185–210. https://doi.org/10.1016/j.precamres.2006.08.008.

Hrachowitz, M., Bohte, R., Mul, M. L., Bogaard, T. A., Savenije, H. H. G., & Uhlenbrook, S. (2011). On the value of combined event runoff and tracer analysis to improve understanding of catchment functioning in a data-scarce semi-arid area. *Hydrology and Earth System Sciences*, *15*, 2007–2024. https://doi.org/10.5194/hess-15-2007-2011

Hrachowitz, M., Savenije, H. H. G., Blöschl, G., McDonnell, J. J., Sivapalan, M., Pomeroy, J. W., … Cudennec, C. (2013). A decade of predictions in ungauged basins (PUB)—A review. *Hydrological Sciences Journal*, *58*, 1–58. https://doi.org/10.1080/02626667.2013.803183.

Hughes, D. (2007). Modelling semi-arid and arid hydrology and water resources—The southern African experience. Chapter 3. In *Hydrological modelling in arid and semi-arid areas*. Cambridge University Press. https://doi.org/10.1017/CBO9780511535734.004

Hughes, D. A., Hannart, P., & Watkins, D. (2003). Continuous baseflow separation from time series of daily and monthly streamflow data. *Water SA*, *29*, 43–48.

Hughes, D. A., Jewitt, G., Mahé, G., Mazvimavi, D., & Stisen, S. (2015). A review of aspects of hydrological sciences research in Africa over the past decade. *Hydrological Sciences Journal*, 1–15. https://doi.org/10.1080/02626667.2015.1072276

ICMA (2010). *The Inkomati catchment management strategy: A first generations catchment management strategy for the Inkomati Water Management Area*. Nelspruit: Inkomati Catchment Management Agency.

Klaus, J., & McDonnell, J. J. (2013). Hydrograph separation using stable isotopes: Review and evaluation. *Journal of Hydrology*, *505*, 47–64. https://doi.org/10.1016/j.jhydrol.2013.09.006.

Kronholm, S. C., & Capel, P. D. (2015). A comparison of high-resolution specific conductance-based end-member mixing analysis and a graphical method for baseflow separation of four streams in hydrologically challenging agricultural watersheds. *Hydrological Processes*, *29*, 2521–2533. https://doi.org/10.1002/hyp.10378

Li, Q., Xing, Z., Danielescu, S., Li, S., Jiang, Y., & Meng, F.-R. (2014). Data requirements for using combined conductivity mass balance and recursive digital filter method to estimate groundwater recharge in a small watershed, New Brunswick, Canada. *Journal of Hydrology*, *511*, 658–664. https://doi.org/10.1016/j.jhydrol.2014.01.073.

Longobardi, A., Villani, P., Guida, D., & Cuomo, A. (2016). Hydro-geo-chemical streamflow analysis as a support for digital hydrograph filtering in a small, rainfall dominated, sandstone watershed. *Journal of Hydrology*, *539*, 177–187. https://doi.org/10.1016/j.jhydrol.2016.05.028.

Love, D., Uhlenbrook, S., Corzo-Perez, G., Twomlow, S., & van der Zaag, P. (2010). Rainfall–interception–evaporation–runoff relationships in a semi-arid catchment, northern Limpopo basin, Zimbabwe. *Hydrological Sciences Journal*, *55*, 687–703. https://doi.org/10.1080/02626667.2010.494010

Mallory, S., & Beater, A. (2009). Inkomati Water Availability Assessment Study (IWAAS). In Department of Water Affairs SA (Ed.), *Hydrology of Crocodile River* (Vol. 1). Pretoria.

Mei, Y., & Anagnostou, E. N. (2015). A hydrograph separation method based on information from rainfall and runoff records. *Journal of Hydrology*, *523*, 636–649. https://doi.org/10.1016/j.jhydrol.2015.01.083.

Middleton, B. J., & Bailey, A. K. (2009). Water resources of South Africa, 2005 study. Water Research Commission.

Miller, M. P., Johnson, H. M., Susong, D. D., & Wolock, D. M. (2015). A new approach for continuous estimation of baseflow using discrete water quality data: Method description and comparison with baseflow estimates from two existing approaches. *Journal of Hydrology*, *522*, 203–210. https://doi.org/10.1016/j.jhydrol.2014.12.039.

Miller, M. P., Susong, D. D., Shope, C. L., Heilweil, V. M., & Stolp, B. J. (2014). Continuous estimation of baseflow in snowmelt-dominated streams and rivers in the upper Colorado River basin: A chemical hydrograph separation approach. *Water Resources Research*, *50*, 6986–6999. https://doi.org/10.1002/2013WR014939

Montanari, A., Young, G., Savenije, H. H. G., Hughes, D., Wagener, T., Ren, L. L., … Belyaev, V. (2013). "Panta Rhei—Everything flows": Change in hydrology and society—The IAHS scientific decade 2013–2022. *Hydrological Sciences Journal*, *58*, 1256–1275. https://doi.org/10.1080/02626667.2013.809088

Nathan, R. J., & McMahon, T. A. (1990). Evaluation of automated techniques for base flow and recession analyses. *Water Resources Research*, *26*, 1465–1473. https://doi.org/10.1029/WR026i007p01465

O'Brien, R. J., Misstear, B. D., Gill, L. W., Johnston, P. M., & Flynn, R. (2014). Quantifying flows along hydrological pathways by applying a new filtering algorithm in conjunction with master recession curve analysis. *Hydrological Processes*, *28*, 6211–6221. https://doi.org/10.1002/hyp.10105

Retief, D. C. H. (2014). Investigating integrated catchment management using a simple water quantity and quality model: A case study of the Crocodile River catchment, South Africa. Rhodes University, pp: 241.

Rimmer, A., & Hartmann, A. (2014). Optimal hydrograph separation filter to evaluate transport routines of hydrological models. *Journal of Hydrology*, *514*, 249–257. https://doi.org/10.1016/j.jhydrol.2014.04.033.

Sahula, A. (2014). Exploring the development of an integrated, participative, water quality management process for the Crocodile River catchment, focusing on the sugar industry. MSc Thesis, Rhodes University, pp: 265.

Saraiva Okello, A. M. L., Masih, I., Uhlenbrook, S., Jewitt, G. P. W., van der Zaag, P., & Riddell, E. (2015). Drivers of spatial and temporal variability of streamflow in the Incomati River basin. *Hydrology and Earth System Sciences*, *19*, 657–673. https://doi.org/10.5194/hess-19-657-2015

Sharpe, M. R., Sohnge, A. P., Zyl, J. S. V., Joubert, D. K., Mulder, M. P., Clubley-Armstrong, A. R., … Taljaard, J. J. (1986). 2530 Barberton. Geoscience Cf (ed.) department of minerals and energy affairs, Government Printer.

Sklash, M. G., & Farvolden, R. N. (1979). The role of groundwater in storm runoff. *Journal of Hydrology*, *43*, 45–65. https://doi.org/10.1016/0022-1694(79)90164-1.

Slaughter, A. R., & Hughes, D. A. (2013). A simple model to separately simulate point and diffuse nutrient signatures in stream flows. *Hydrology Research*, *44*, 538–553.

Soulsby, C., Rodgers, P. J., Petry, J., Hannah, D. M., Malcolm, I. A., & Dunn, S. M. (2004). Using tracers to upscale flow path understanding in mesoscale

mountainous catchments: Two examples from Scotland. *Journal of Hydrology*, *291*, 174–196. https://doi.org/10.1016/j.jhydrol.2003.12.042.

Stats S (2016). Mid-year population estimates 2016. Statistics South Africa.

Stewart, M. K. (2015). Promising new baseflow separation and recession analysis methods applied to streamflow at Glendhu catchment, New Zealand. *Hydrology and Earth System Sciences*, *19*, 2587–2603. https://doi.org/10.5194/hess-19-2587-2015

Tallaksen, L. M. (1995). A review of baseflow recession analysis. *Journal of Hydrology*, *165*, 349–370. https://doi.org/10.1016/0022-1694(94)02540-R.

Tetzlaff, D., Buttle, J., Carey, S. K., McGuire, K., Laudon, H., & Soulsby, C. (2015). Tracer-based assessment of flow paths, storage and runoff generation in northern catchments: A review. *Hydrological Processes*, *29*, 3475–3490. https://doi.org/10.1002/hyp.10412

Tetzlaff, D., & Soulsby, C. (2008). Sources of baseflow in larger catchments—Using tracers to develop a holistic understanding of runoff generation. *Journal of Hydrology*, *359*, 287–302. https://doi.org/10.1016/j.jhydrol.2008.07.008.

Tetzlaff, D., Waldron, S., Brewer, M. J., & Soulsby, C. (2007). Assessing nested hydrological and hydrochemical behaviour of a mesoscale catchment using continuous tracer data. *Journal of Hydrology*, *336*, 430–443.

Uhlenbrook, S., Frey, M., Leibundgut, C., & Maloszewski, P. (2002). Hydrograph separations in a mesoscale mountainous basin at event and seasonal timescales. *Water Resources Research*, *38*, 31–31-31-14. https://doi.org/10.1029/2001wr000938

Uhlenbrook, S., & Hoeg, S. (2003). Quantifying uncertainties in tracer-based hydrograph separations: A case study for two-, three- and five-component hydrograph separations in a mountainous catchment. *Hydrological Processes*, *17*, 431–453. https://doi.org/10.1002/hyp.1134

van Eekelen, M. W., Bastiaanssen, W. G. M., Jarmain, C., Jackson, B., Ferreira, F., van der Zaag, P., … Luxemburg, W. M. J. (2015). A novel approach to estimate direct and indirect water withdrawals from satellite measurements: A case study from the Incomati basin. *Agriculture, Ecosystems & Environment*, *200*, 126–142. https://doi.org/10.1016/j.agee.2014.10.023.

van Wyk, E., van Tonder, G., & Vermeulen, D. (2011). Characteristics of local groundwater recharge cycles in South African semi-arid hard rock terrains-rainwater input. *Water SA*, *37*, 147–154.

Van Wyk, E., Van Tonder, G., & Vermeulen, D. (2012). Characteristics of local groundwater recharge cycles in South African semi-arid hard rock terrains: Rainfall-groundwater interaction. *Water SA*, *38*, 747–754.

Wenninger, J., Uhlenbrook, S., Lorentz, S., & Leibundgut, C. (2008). Identification of runoff generation processes using combined hydrometric, tracer and geophysical methods in a headwater catchment in South Africa. *Hydrological Sciences Journal-Journal Des Sciences Hydrologiques*, *53*, 65–80.

Wheater, H., Sorooshian, S., & Sharma, K. D. (2008). *Hydrological modelling in arid and semi-arid areas*. Cambridge, UK: Cambridge University Press.

Zhang, R., Li, Q., Chow, T. L., Li, S., & Danielescu, S. (2013). Baseflow separation in a small watershed in New Brunswick, Canada, using a recursive digital filter calibrated with the conductivity mass balance method. *Hydrological Processes*, *27*, 2659–2665. https://doi.org/10.1002/hyp.9417

SUPPORTING INFORMATION

Additional Supporting Information may be found online in the supporting information tab for this article.

How to cite this article: Saraiva Okello AML, Uhlenbrook S, Jewitt GPW, Masih I, Riddell ES, Van der Zaag P. Hydrograph separation using tracers and digital filters to quantify runoff components in a semi-arid mesoscale catchment. *Hydrological Processes*. 2018;32:1334–1350. https://doi.org/10.1002/hyp.11491